Food and Chemical Toxicology 132 (2019) 110651

Contents lists available at ScienceDirect

Food and Chemical Toxicology

journal homepage: www.elsevier.com/locate/foodchemtox

Renal protective effects of aloin in a mouse model of sepsis

Wonhwa Lee[a,1], Gil-Saeng Jeong[b,1], Moon-Chang Baek[c], Sae-Kwang Ku[d,**], Jong-Sup Bae[a,*]

[a] College of Pharmacy, CMRI, Research Institute of Pharmaceutical Sciences, BK21 Plus KNU Multi-Omics Based Creative Drug Research Team, Kyungpook National University, Daegu, 41566, Republic of Korea
[b] College of Pharmacy, Keimyung University, Daegu, 42601, Republic of Korea
[c] Department of Molecular Medicine, CMRI, School of Medicine, Kyungpook National University, Daegu, 41944, Republic of Korea
[d] Department of Histology and Anatomy, College of Korean Medicine, Daegu Haany University, Gyeongsan-si, 38610, Republic of Korea

ARTICLE INFO

Keywords:
Aloin
Sepsis
Antioxidant
Renal injury
Renal toxicity

ABSTRACT

Aloin is the major anthraquinone glycoside obtained from the *Aloe* species and exhibits anti-inflammatory and anti-oxidative activities. However, the renal protective effects of aloin and underlying molecular mechanism remain unclear. This study was initiated to determine whether aloin could modulate renal functional damage in a mouse model of sepsis and to elucidate the underlying mechanisms. The potential of aloin treatment to reduce renal damage induced by cecal ligation and puncture (CLP) surgery in mice was measured by assessment of serum creatinine, blood urea nitrogen (BUN), lipid peroxidation, total glutathione, glutathione peroxidase activity, catalase activity, and superoxide dismutase activity. Post-treatment with aloin resulted in a significant reduction in the deleterious renal functions by CLP, such as elevated BUN, creatinine, and urine protein. Moreover, aloin inhibited nuclear factor-κB activation and reduced the induction of nitric oxide synthase and excessive production of nitric acid. Aloin treatment also reduced the plasma levels of interleukin-6 and tumor necrosis factor-α, reduced lethality due to CLP-induced sepsis, increased lipid peroxidation, and markedly enhanced the antioxidant defense system by restoring the levels of superoxide dismutase, glutathione peroxidase, and catalase in kidney tissues. Our study suggested that aloin protects mice against sepsis-triggered renal injury.

1. Introduction

Sepsis is defined as a systemic inflammatory response syndrome caused by infection and is a common cause of morbidity and mortality, despite recent advances in antibiotic therapy and intensive care (Russell, 2006). In the past 30 years, sepsis has become one of the major causes of hospital admission and medical expenses (Singer et al., 2016). Although activation of cytokines is part of the host defense response to infection, excessive production and secretion of cytokines can cause widespread tissue injury and organ failure (Chaudhry et al., 2013). Septic conditions activate inducible nitric oxide synthase (iNOS) and increase the plasma concentration of nitric oxide (NO), which ultimately leads to cytotoxicity (Parratt, 1998; Symeonides and Balk, 1999). Sepsis is also known to enhance the synthesis of reactive oxygen species (ROS) such as superoxide anions and hydrogen peroxide (Parratt, 1998; Symeonides and Balk, 1999). The excessive production of ROS can cause significant oxidative stress as indicated by a decrease in endogenous antioxidant defenses and lipid peroxidation. The rate of organ failure due to sepsis can be diminished by reduction of inflammatory cytokines and inhibition of iNOS activity (Draisma et al., 2010; Parratt, 1998; Symeonides and Balk, 1999). Since interventions that reduce the production or the effect of ROS have been shown to have beneficial effects on sepsis (Cadenas and Cadenas, 2002; Vincent et al., 2000), agents that can decrease cytokine production and ROS might also prevent or lessen the pathological cascade of inflammation caused by sepsis.

Natural substances have been traditionally administered to treat or prevent various diseases, such as cancer and infectious diseases (Lu et al., 2004; Zhang et al., 2013, 2017). Aloin is the major anthraquinone glycoside obtained from the *Aloe* species. It is well known that aloin has anti-tumor (Chen et al., 2007; Esmat et al., 2005, 2006; Niciforovic et al., 2007; Tabolacci et al., 2010), anti-viral (Li et al., 2014; Lin et al., 2008), hepato-protective (Arosio et al., 2000; Woo et al., 2002), anti-oxidative (Beppu et al., 2003; Tao et al., 2014; Wan et al., 2017),

* Corresponding author. College of Pharmacy, Kyungpook National University, 80 Daehak-ro, Buk-gu, Daegu, 41566, Republic of Korea.
** Corresponding author. Department of Histology and Anatomy, College of Korean Medicine, Daegu Haany University, 1 Haanydaero, Gyeongsan-si, 38610, Republic of Korea.
E-mail addresses: gucci200@hanmail.net (S.-K. Ku), baejs@knu.ac.kr (J.-S. Bae).
[1] First two authors contributed equally to this work.

https://doi.org/10.1016/j.fct.2019.110651
Received 27 March 2019; Received in revised form 23 June 2019; Accepted 26 June 2019
Available online 27 June 2019
0278-6915/

immunomodulatory and anti-inflammatory (Park et al., 2009; Seo et al., 2014; Silva et al., 2014; Yu et al., 2006) activities. However, to our knowledge, the possible protective effects of aloin against renal damage have not been studied. Based on previous reports on the renal-damaging potential of cecal ligation and puncture (CLP)-induced septic model (Buras et al., 2005; Doi et al., 2009), and the beneficial activities of aloin described above, we hypothesized that aloin treatment may inhibit the development of CLP-induced renal injury. To clarify its protective role, we analyzed the effects of aloin on CLP-induced renal damage by assessment of renal damage and oxidative markers and underlying mechanism.

2. Materials and methods

2.1. Reagents

Aloin was purchased from Sigma (St. Louis, MO). Cudratricusxanthone A (CTXA), as a positive control, was prepared as previously described (Lee et al., 2017). Nuclear and cytoplasmic protein extraction reagent kits were obtained from Thermo Scientific Company (Rockford, lL). Antibodies against iNOS, IκB, phospho-IκB, nuclear factor (NF)-κB, phosphor–NF–κB, Lamin-B, and β-actin were purchased from Cell Signaling Technology (Danvers, MA).

2.2. Animals and cecal ligation and puncture

Male C57BL/6 mice (6–7 weeks old) were obtained from Orient Bio Co. (Sungnam, Republic of Korea) and were given a 12 d acclimatization period. The mice were housed under controlled temperature (20–25 °C) and humidity conditions (40–45% RH), with a 12 h light:12 h dark cycle. They were fed a normal rodent pellet diet and had *ad libitum* access to water during acclimatization. To induce sepsis, the mice were first anesthetized with Zoletil (tiletamine and zolazepam, 1:1 mixture, 30 mg/kg) and Rompum (xylazine, 10 mg/kg). Sepsis was induced using cecal ligation and puncture (CLP) as previously described (Kim et al., 2019; Lee and Bae, 2019). As controls, sham-operated animals were used: in these mice, the cecum was exposed, but not ligated or punctured, and then returned to the abdominal cavity. Animals were randomly divided into 9 treatment groups (n = 10 each): sham-operated control; aloin-only (12.4 mg/kg body weight) in 0.5% DMSO; CTXA-only (0.294 mg/kg body weight) in 0.5% DMSO; CLP surgery only; CLP + aloin (1.6, 3.1, 6.2, or 12.4 mg/kg body weight); and CLP + CTXA (0.294 mg/kg body weight). For the CLP-induced septic lethality experiments, animals were randomly divided into 5 treatment groups (n = 20 each): sham-operated control; CLP surgery only; CLP + aloin in 0.5% DMSO (12.4 or 24.8 mg/kg body weight); and CLP + CTXA in 0.5% DMSO (0.294 mg/kg body weight). Aloin or CTXA was intravenously injected at 12 h after CLP and again at 50 h after CLP. Animal survival was monitored every 12 h for 132 h after CLP. Blood and organ samples were collected 4 days after aloin injection for functional assays. This protocol was approved by the Animal Care Committee at Kyungpook National University prior to conducting the study (IRB No. KNU, 2017–102).

2.3. Sample preparation

Four days after aloin injection, the mice were anesthetized as described above and sacrificed. Blood samples were collected from the posterior vena cava and allowed to clot. Serum was separated by centrifugation at 4000 rpm for 10 min, stored at −80 °C until analyzed and was used for the assessment of plasma BUN and creatinine levels. Kidney samples were immediately removed and weighed. The kidneys were then minced with scissors and homogenized in 0.1 M phosphate buffer saline (pH 7.4); the tissue was fractionated under refrigeration by centrifugation at 10,000 × *g* for 10 min. The homogenate was stored at −80 °C until analyzed in the various biochemical assays. Protein concentrations were determined using the Bradford assay.

2.4. Evaluation of nephrotoxicity and lactate dehydrogenase

Renal dysfunction was assessed by measuring the changes in levels of BUN and creatinine, and of protein in urine. BUN, creatinine, and lactate dehydrogenase (LDH), another important marker of tissue injury, were measured using commercial assay kits (Pointe Scientific, Linclon Park, MI). Urine samples were collected from each animal using a metabolic cage at 12 h after CLP surgery and the supernatant was obtained. Urinary protein concentrations were determined by the Bradford assay, using BSA as the protein standard.

2.5. Plasma nitrite/nitrate determination

Nitrite and nitrate concentrations in the plasma were determined using Griess reagents and vanadium solution (VCl_3) as previously described (Miranda et al., 2001). Briefly, 100 μL of VCl_3 were added to 100 μL of sample, immediately followed by Griess reagents (0.1% N-1-naphthylethylenediamine dihydrochloride and 1% sulfanilamide in 5% phosphoric acid). After 30 min of color development, absorbance was determined by measuring optical density (OD) at 540 nm using a microplate reader (Tecan Austria GmbH, Austria). Concentrations were determined by comparing absorptions with those of a standard curve of sodium nitrite.

2.6. ELISA for tumor necrosis factor (TNF)-α, interleukin (IL)-6, and heme oxygenase-1 (HO-1)

The plasma concentrations of IL-6, TNF-α, HO-1 were determined using ELISA kits (R&D Systems, Minneapolis, MN). Values were measured using an ELISA plate reader (Tecan, Austria GmbH, Austria).

2.7. Renal myeloperoxidase activity

Renal myeloperoxidase (MPO) activity was used as a quantitative indicator for neutrophil influx into the kidney; MPO activity was measured using ELISA kits (Abcam, UK).

2.8. Evaluation of oxidative stress markers

Lipid peroxidation was determined using a method to measure the formation of thiobarbituric acid reactive substances (TBARSs). The level of malondialdehyde (MDA) in kidney tissue was measured spectrophotometrically using an OxiSelect TBARS assay kit (Cell Biolabs, San Diego, CA). MDA values were expressed as nM/mg protein. Total glutathione (GSH) contents of kidney tissue were measured as described previously (Beutler et al., 1963). A tissue homogenate was prepared, and then samples were added to metaphosphoric acid and allowed to stand for 5 min to precipitate proteins. Phosphate buffer and 5,5′-dithiobis-2-nitro-benzoic acid were added for color development. GSH was determined by measuring absorbance at 415 nm and absolute concentrations were calculated using a GSH standard (Sigma Aldrich, St. Louis, MO). Values of total GSH were expressed as nM/mg protein. Superoxide dismutase (SOD) activity was measured using a SOD assay kit (Fluka). Values of SOD were expressed as U/mg protein. Glutathione peroxidase (GSH-Px) activity was determined using the cellular activity assay kit CGP-1 (Sigma Aldrich). Values of GSH-Px were expressed as U/mg protein. Catalase activity (CAT) was determined by a CAT assay kit (Sigma Aldrich) using the decomposition rate of the substrate H_2O_2 as determined at 240 nm. Total CAT values were expressed as U/mg protein.

2.9. RNA isolation and real-time quantitative RT-PCR

Total RNA was isolated using RNeasy (Qiagen, Valencia, CA). An

aliquot (5 μg) of extracted RNA was reverse transcribed into first-strand cDNA with a PX2 Thermal Cycler (Thermo Scientific), using 200 U/μL M-MLV reverse-transcriptase (Invitrogen, Grand Island, NY) and 0.5 mg/μL of oligo (dT)-adapter primer (Invitrogen, Grand Island, NY) in a 20-μL reaction mixture. Real-time PCR for COX-2, p38, JNK, and GAPDH was performed with a Mini Opticon Real-Time PCR System (Bio-Rad, Hercules, CA), using iQ SYBR Green Supermix (Bio-Rad, Hercules, CA). The sequences of the primers were as follows: for COX-2, sense 5′-GCAAATCCTTGCTGTTCCAATC-3′ and antisense 5′-GGAGAA GGCTTCCCAGCTTTTG-3′; for p38 sense 5′-GGA GAA GAT GCT CGT TTT GGA-3′ and antisense 5′-TTG GTC AAG GGG TGG TGG-3; for JNK sense 5′-CGT CTG GTG GAA GGA GAG AG-3′ and antisense 5′-TAA TAA CGG GGG TGG AGG AT-3′; for SOD1 sense 5′-CCA GTG CAG GAC CTC ATT TT-3′ and antisense 5′-CAC CTT TGC CCA AGT CAT CT-3′; for GSH-Px1 sense 5′-GGT TCG AGC CCA ATT TTA CA-3′ and antisense 5′-CCC ACC AGG AAC TTC TCA AA-3′; for CAT sense 5′-GCT GAG AAG CCT AAG AAC GCA AT-3′ and antisense 5′-CCC TTC GCA GCC ATG TG-3′; for GAPDH, sense 5′-CGG AGT CAA CGG ATT TGG TCG TAT -3′ and antisense 5′-AGC CTT CTC CAT GGT GGT GAA GAC-3′. The PCR settings were as follows: initial denaturation at 95 °C was followed by 35 cycles of amplification for 15 s at 95 °C and 20 s at 60 °C, with subsequent melting curve analysis, increasing the temperature from 72 to 98 °C. Quantification of gene expression was calculated relative to GAPDH.

2.10. Cell culture

Primary mouse kidney endothelial cells were obtained from Cell Biologics Company (Chicago, IL) and maintained according to the instructions. These cells were grown in endothelial cell basal medium (Cell Biologics Company) containing10% feta bovine serum (FBS) and the endothelial cell growth supplements provided by the company. Cells were used between passages 3 and 5 in culture. The effects of aloin on the induction of HO-1 and on the nuclear accumulation of Nrf2 in mouse kidney endothelial cells were determined.

2.11. Western blots from renal tissue or cell lysates

Kidney samples were homogenized with radioimmunoprecipitation (RIPA) buffer containing protease inhibitors; equal amounts of protein were separated by SDS-PAGE (10%) and were electroblotted overnight onto an Immobilon membrane (Millipore, Billerica, MA). Or, nuclear and cytoplasmic protein was prepared using extraction kit (Thermo Scientific Company, Rockford, lL). The membranes were blocked for 1 h with 5% low-fat milk-powder TBS (50 mM Tris-HCl, pH 7.5, 150 mM NaCl) containing 0.05% Tween 20 and were then incubated with primary antibodies for iNOS, IκB, phospho-IκB, phospho–NF–κB, NF-κB, nuclear factor erythroid-2 related factor 2 (Nrf2), Lamin-B, and β-actin, at 4 °C overnight. Subsequently, the membranes were incubated with horseradish-peroxidase-conjugated secondary antibody, and enhanced chemiluminescence (ECL) detection was performed according to the manufacturer's instructions.

2.12. Hematoxylin & eosin staining and histopathological examination

Male C57BL/6 mice were subjected to CLP and were administered aloin (12.4 mg/kg, i.v.) at 12 h and 50 h after CLP (n = 5). At 96 h after CLP, the mice were euthanized. To analyze the phenotypic change in the kidney, samples were removed from each mouse, washed three times in PBS (pH 7.4) to remove the remaining blood, and fixed in 4% formaldehyde solution (Junsei, Tokyo, Japan) in PBS for 20 h at 4 °C. After fixation, the samples were dehydrated using an ethanol series, embedded in paraffin, sectioned into 4-μm slices, and placed on a slide. The slides were deparaffinized in a 60 °C oven, rehydrated, and stained with hematoxylin (Sigma). To remove over-staining, the slides were quickly dipped three times in 0.3% acid alcohol and counterstained with eosin (Sigma). Over-staining was then removed by washes in an ethanol series and xylene, and the samples were placed under a coverslip. Light microscopic analysis of the specimens was performed by a blinded observer who evaluated pulmonary architecture, tissue edema, and infiltration of the inflammatory cells by a previously defined method (Ozdulger et al., 2003).

2.13. Statistical analysis

All experiments were performed independently at least three times. Values are expressed as means ± standard deviation (SD). The statistical significance of differences between test groups was evaluated using SPSS for Windows, version 16.0 (SPSS, Chicago, IL). Statistical relevance was determined by one-way analysis of variance (ANOVA) and Tukey's post-hoc test. *P* values less than 0.05 were considered to indicate significance.

3. Results

3.1. Effects of aloin on CLP-induced renal tissue injury

Previous reports showed that treatment of cells or mice with aloin inhibited LPS-induced expression of inflammatory cytokines and had protective effects against oxidative damages which contributes to vascular inflammation (Lam et al., 2007; Lee et al., 2019; Luo et al., 2018). In those studies, aloin was used from at 100 μM–400 μM in human endothelial cells and from at 3.1 mg/kg to 12.4 mg/kg in mice. As the average circulating blood volume for mice is 72 mL/kg (Diehl et al., 2001) and the average weight of mouse used was 27 g, the average blood volume was 2 mL. Hence, the amount of injected aloin (1.6, 3.1, 6.2, or 12.4 mg/kg) yielded a concentration of 50, 100, 200, or 400 μM in the peripheral blood. Therefore, in this study, aloin was also used from 1.6 to 12.4 mg/kg. Recently we reported the renal protective effect of CTXA against CLP-induced kidney injury and septic lethality (Lee et al., 2017). The ameliorative effects of CTXA were associated with down-regulation down-regulation of TNF-α and IL-6 productions as well as inducible nitric oxide synthase expression and lowered NO by blocking NF-kB pathway. These effects were accompanied by enhancing antioxidant defense and decreased lipid peroxidation in the kidney and plasma *in vivo* (Lee et al., 2017). Therefore, CTXA was used as a positive control (Lee et al., 2017).

The effects of CLP surgery on nephrotoxic markers are shown in Table 1: plasma levels of BUN and creatinine, and protein levels in urine were significantly higher on the fourth day after CLP surgery than in the sham-operated group. Sham operation or administration of aloin only to mice did not result in any obvious changes in plasma levels of BUN and creatinine, or of protein in urine. The increased levels of BUN and creatinine, and of protein in urine after surgery were not blocked by a single administration of aloin (1.6–12.4 mg/kg, 12 h after CLP, data not shown). Thus, we administered two equal doses of aloin, one at 12 h after CLP and the other at 50 h after CLP. We found that aloin decreased BUN, creatinine, and protein in urine levels (Table 1). Another important marker of tissue injury, LDH, was also reduced by aloin in CLP-operated mice (Table 1).

3.2. Effects of aloin on plasma nitrite and nitrate production after CLP surgery

The effects of aloin treatment on inflammatory response in kidney tissue were investigated *in vivo* by measuring plasma nitrite and nitrate levels (stable end products of NO). In sham-operated and aloin-only mice, the levels of plasma NO did not significantly change (Table 2). However, CLP surgery caused an approximately 7.3-fold increase in mouse plasma NO production with respect to that in control mice (Table 2). Post-surgery treatment with aloin resulted in NO levels being up to 43% lower than those in the CLP group (Table 2).

Table 1
Effects of aloin treatment on plasma levels of BUN and creatinine and urine level of protein in CLP-operated mice.[a]

	BUN (mg/dL)	Creatinine (mg/dL)	Urine protein (mg/12 h)	LDH (U/dL)
Sham	15.9 ± 1.2	0.105 ± 0.015	2.1 ± 0.19	305 ± 18.5
Aloin (12.4 mg/kg)	16.2 ± 1.1	0.119 ± 0.019	2.2 ± 0.21	331 ± 25.2
CTXA (0.294 mg/kg)	16.4 ± 1.3	0.125 ± 0.021	2.3 ± 0.15	295 ± 21.4
CLP	75.2 ± 4.8	0.435 ± 0.032	13.5 ± 1.05	3850 ± 315.5
CLP + Aloin (1.6 mg/kg)	75.9 ± 4.3	0.439 ± 0.041	12.9 ± 0.87	3789 ± 221.1
CLP + Aloin (3.1 mg/kg)	63.1 ± 3.9*	0.318 ± 0.031*	9.4 ± 0.74*	2751 ± 175.3*
CLP + Aloin (6.2 mg/kg)	45.3 ± 2.9*	0.249 ± 0.025*	6.5 ± 0.39*	1781 ± 141.2*
CLP + Aloin (12.4 mg/kg)	32.2 ± 3.5*	0.219 ± 0.029*	4.1 ± 0.23*	1321 ± 115.3*
CLP + CTXA (0.294 mg/kg)	35.1 ± 3.1*	0.229 ± 0.016*	4.3 ± 0.21*	1258 ± 86.2*

Sham, sham-operated mice; aloin, mice treated with aloin (12.4 mg/kg body weight) at 12 and 50 h; CTXA, mice treated with CTXA (0.294 mg/kg body weight) at 12 and 50 h; CLP, CLP-operated mice; aloin + CLP, mice treated with aloin at 12 and 50 h after CLP surgery; CTXA + CLP, mice treated with CTXA at 12 and 50 h after CLP surgery.
* $p < 0.05$ as compared to CLP.
[a] Each value represents the mean ± SD (n = 10).

3.3. Effects of aloin on plasma TNF-α, IL-6, and MPO levels

The effects of aloin on CLP-induced inflammatory responses were investigated through measurement of plasma levels of TNF-α and IL-6. CLP surgery significantly increased plasma TNF-α and IL-6 levels; post-surgery treatment with aloin inhibited these increases (Table 2). Plasma concentrations of TNF-α and IL-6 were lower by 61 and 69%, respectively, in CLP + aloin (12.4 mg/kg) group than in the CLP group. Next, we determined the effects of aloin treatment on infiltration of neutrophils after CLP surgery. Kidney tissues were collected, homogenized, and centrifuged, and supernatants were assayed for MPO level by ELISA. MPO activity can act as an indicator of renal infiltration by neutrophils. We identified a marked increase in MPO level after CLP surgery (Table 2), which was associated with nephritis. Treatment with aloin post-surgery resulted in a significantly lower MPO concentration in renal tissues than that in the CLP-operated mice. Moreover, during inflammatory response, inflammatory mediator proteins expression and MAPKs signaling pathways are closely involved in the regulation of inflammatory response. Therefore, we determined the effects of aloin on the transcriptional regulation of cyclooxygenase (COX)-2 and mitogen-activated protein kinase (MAPK) such as p38 and janus kinase (JNK). Data showed that aloin inhibited CLP-mediated expressions of COX-2, p38, and JNK (Table 3).

3.4. Effect of aloin on kidney tissue MDA

MDA concentration is an indicator of lipid peroxidation levels. In kidney tissues of CLP-operated mice, a significant increase in MDA levels was present (Table 4). Treatment with aloin post-surgery led to significantly lower MDA levels than those in the control group.

3.5. Effect of aloin on total GSH and activities of antioxidant enzymes in renal tissues

To test the effect of aloin on CLP-induced oxidative stress, we analyzed the activities of the antioxidant GSH and the oxidative stress associated enzymes superoxide dismutase (SOD), glutathione peroxidase (GSH-Px), and catalase (CAT). Total GSH levels and the activities of SOD, GSH-Px, and CAT were similar in the aloin -only and sham-operated groups. In contrast, total GSH levels and renal activities of all three enzymes were reduced in the CLP mice. However, post-surgery treatment with aloin increased total GSH and renal enzyme activities (Table 4). Moreover, aloin suppressed the transcriptional expression levels of SOD, GSH-Px, and CAT by CLP (Table 3). Noting that nuclear factor erythroid-2 related factor 2 (Nrf2) is a potential pathway to protective responses against oxidative stress, and heme oxygenase-1 (HO-1) is one of the most important enzymes for antioxidant pathway (Agca et al., 2014; Yu et al., 2013). Therefore, we determined the effects of aloin on the induction of HO-1 and on the nuclear accumulation of Nrf2 in mouse kidney endothelial cells. To do this, primary mouse endothelial cells were incubated with aloin for 16 h. And then, the expressions of HO-1 in extracted protein were measured by ELISA (Fig. 1A) or the expressions of Nrf2 in separated cytosolic and nuclear fractions were measured by western blotting (Fig. 1B). Data showed that HO-1 protein expression was induced by aloin (Fig. 1A) and aloin mediated the translocation of Nrf2 from the cytosol to nucleus in a concentration-dependent manner (Fig. 1B). Therefore, these results indicate that the Nrf2/HO-1 signaling axis plays an important role in the anti-oxidant effects of aloin.

Table 2
Effects of aloin treatment on NO, TNF-α, IL-6 levels and renal MPO activity in CLP-operated mice.[a]

	NO (μM)	TNF-α (pg/mL)	IL-6 (pg/mL)	MPO (U/g tissue)
Sham	30.21 ± 3.05	131.38 ± 11.32	0.97 ± 0.08	0.71 ± 0.08
Aloin (12.4 mg/kg)	32.17 ± 3.29	135.12 ± 13.21	0.83 ± 0.07	0.82 ± 0.09
CTXA (0.294 mg/kg)	34.21 ± 2.23	138.47 ± 10.18	0.57 ± 0.06	0.78 ± 0.08
CLP	219.31 ± 19.27	525.15 ± 38.27	89.32 ± 6.35	3.65 ± 1.21
CLP + Aloin (1.6 mg/kg)	218.23 ± 18.38	519.53 ± 42.19	88.85 ± 3.91	3.38 ± 1.39
CLP + Aloin (3.1 mg/kg)	168.29 ± 14.21*	395.38 ± 32.69*	65.19 ± 5.32*	2.51 ± 0.23*
CLP + Aloin (6.2 mg/kg)	131.33 ± 10.08*	289.54 ± 22.38*	33.69 ± 3.11*	1.89 ± 0.21*
CLP + Aloin (12.4 mg/kg)	95.62 ± 7.32*	202.31 ± 19.82*	27.25 ± 2.27*	1.71 ± 0.17*
CLP + CTXA (0.294 mg/kg)	110.28 ± 9.18*	219.28 ± 15.27*	28.37 ± 1.74*	1.68 ± 0.19*

Sham, sham-operated mice; aloin, mice treated with aloin (12.4 mg/kg body weight) at 12 and 50 h; CTXA, mice treated with CTXA (0.294 mg/kg body weight) at 12 and 50 h; CLP, CLP-operated mice; aloin + CLP, mice treated with aloin at 12 and 50 h after CLP surgery; CTXA + CLP, mice treated with CTXA at 12 and 50 h after CLP surgery.
* $p < 0.05$ as compared to CLP.
[a] Each value represents the mean ± SD (n = 10).

Table 3
Effect of aloin on the expressions of COX-2, p38, JNK MAPK, SOD, GSH-Px, and CAT mRNA.[a]

	COX-2 mRNA (fold change)	p38 mRNA (fold change)	JNK mRNA (fold change)	SOD 1 mRNA (fold change)	GSH-Px mRNA (fold change)	CAT mRNA (fold change)
Sham	1	1	1	1	1	1
Aloin (12.4 mg/kg)	1.08 ± 0.05	1.11 ± 0.08	1.05 ± 0.03	1.12 ± 0.05	1.08 ± 0.07	1.19 ± 0.02
CTXA (0.294 mg/kg)	1.05 ± 0.03	1.08 ± 0.05	1.07 ± 0.02	1.10 ± 0.04	1.05 ± 0.03	1.13 ± 0.05
CLP	10.71 ± 1.12	9.85 ± 0.75	8.23 ± 0.82	6.88 ± 0.52	4.25 ± 0.32	6.25 ± 0.31
CLP + Aloin (1.6 mg/kg)	10.92 ± 1.21	9.85 ± 0.62	8.31 ± 0.72	6.75 ± 0.62	4.19 ± 0.37	6.31 ± 0.37
CLP + Aloin (3.1 mg/kg)	7.12 ± 0.68*	6.12 ± 0.55*	5.82 ± 0.62*	5.37 ± 0.41*	3.83 ± 0.32*	4.42 ± 0.41*
CLP + Aloin (6.2 mg/kg)	5.37 ± 0.47*	5.29 ± 0.47*	3.59 ± 0.42*	4.29 ± 0.32*	2.78 ± 0.22*	3.36 ± 0.32*
CLP + Aloin (12.4 mg/kg)	3.29 ± 0.25*	3.11 ± 0.32*	2.75 ± 0.32*	3.52 ± 0.29*	1.92 ± 0.22*	2.37 ± 0.15*
CLP + CTXA (0.294 mg/kg)	3.49 ± 0.31*	3.27 ± 0.27*	2.82 ± 0.22*	3.71 ± 0.25*	1.85 ± 0.15*	2.17 ± 0.17*

Sham, sham-operated mice; aloin, mice treated with aloin (12.4 mg/kg body weight) at 12 and 50 h; CTXA, mice treated with CTXA (0.294 mg/kg body weight) at 12 and 50 h; CLP, CLP-operated mice; aloin + CLP, mice treated with aloin at 12 and 50 h after CLP surgery; CTXA + CLP, mice treated with CTXA at 12 and 50 h after CLP surgery.

* $p < 0.05$ as compared to CLP.

[a] Each value represents the mean ± SD (n = 10).

3.6. Effect of aloin on the levels of the renal proteins iNOS, IκB and NF-κB and on cellular toxicity

To explore the mechanisms responsible for mediating the anti-inflammatory effects of aloin, we measured the levels of iNOS, IκB, and NF-κB proteins in kidney tissues of the mice. iNOS protein levels were low in kidney homogenates obtained from the control groups, but were significantly elevated in CLP-operated mice. Post-surgery treatment with aloin significantly reduced this increase in iNOS (Fig. 2A). Next, we investigated whether aloin could inhibit the CLP-induced degradation of IκB and prevent the translocation of the subunit of NF-κB p65 from the cytosol to the nucleus. As shown in Fig. 2, the translocation of nuclear factor (NF)-κB p65 to nucleus and activation of NF-κB p65 in nucleus and inhibitory kappa B (IκB) phosphorylation in kidney significantly increased after CLP. Moreover, aloin administration after CLP decreased NF-κB p65 activation and IκB phosphorylation compared with the CLP group. In addition, degradation of IκB was lower in the aloin + CLP group than in the CLP-only group (Fig. 2B).

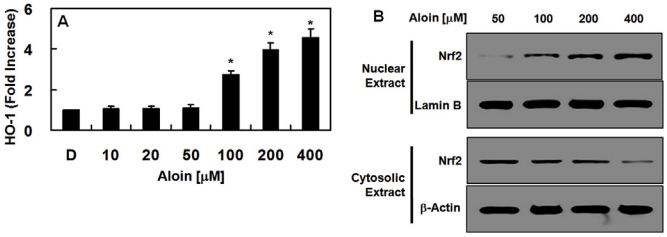

Fig. 1. Effects of aloin treatment on the expression levels of HO-1 in mouse kidney endothelial cells and on the nuclear accumulation of Nrf2. (A) Mouse kidney endothelial cells were harvested after treatment with aloin (0–400 μM) for 16 h. The extracted proteins were subjected to ELISA for HO-1 expression. (B) Mouse kidney endothelial cells were harvested after treatment with aloin (5–500 μM) for 16 h, and their cytosolic and nuclear fractions were extracted using a separation kit. The extracted proteins were subjected to western blotting for Nrf2. The images are representative of results obtained from three different experiments. D = 0.2% DMSO is the vehicle control. *$p < 0.05$ versus DMSO (A).

3.7. Effect of aloin in CLP-induced septic lethality

To evaluate whether the renal protective responses identified after aloin treatment influenced the survival rate of mice with CLP-induced sepsis, we administered two equal doses of aloin (12.4 mg/kg), one at 12 h after CLP and the other at 50 h after CLP. The aloin treatment increased the rate of survival of mice with sepsis (60%), according to a Kaplan-Meier survival analysis ($p < 0.0001$, Fig. 3A). However, there were no additional beneficial effects of aloin at 24.8 mg/kg compared to aloin at 12.4 mg/kg (Fig. 3A). The marked improvement in survival rate achieved by the treatment suggested that aloin might be of value in therapies for severe vascular inflammatory diseases, such as sepsis and septic shock.

3.8. Protective effect of aloin in CLP-induced renal injury

We determined the effects of aloin on CLP-induced renal injury to confirm the protective activity of aloin in CLP-induced death by

Table 4
Effects of aloin treatment on MDA level and the activities of renal antioxidant enzymes in CLP-operated mice.[a]

	MDA (nM/mg protein)	GSH (nM/mg protein)	SOD (U/mg protein)	GSH-Px (U/mg protein)	CAT (U/mg protein)
Sham	172.37 ± 13.25	25.21 ± 2.23	1.05 ± 0.02	2.25 ± 0.21	4.37 ± 0.31
Aloin (12.4 mg/kg)	180.23 ± 14.19	26.02 ± 2.05	1.11 ± 0.04	2.37 ± 0.23	4.49 ± 0.37
CTXA (0.294 mg/kg)	185.08 ± 12.08	25.89 ± 2.38	1.08 ± 0.02	2.41 ± 0.18	4.31 ± 0.26
CLP	322.12 ± 23.82	17.12 ± 1.57	0.69 ± 0.06	1.31 ± 0.13	2.75 ± 0.28
CLP + Aloin (1.6 mg/kg)	320.38 ± 25.37	17.29 ± 1.71	0.71 ± 0.07	1.35 ± 0.17	2.81 ± 0.28
CLP + Aloin (3.1 mg/kg)	272.72 ± 20.38*	19.25 ± 1.62*	0.85 ± 0.08*	1.69 ± 0.15*	3.39 ± 0.33*
CLP + Aloin (6.2 mg/kg)	234.85 ± 17.52*	21.47 ± 2.39*	0.87 ± 0.06*	1.89 ± 0.17*	3.87 ± 0.33*
CLP + Aloin (12.4 mg/kg)	213.53 ± 15.71*	23.29 ± 2.37*	0.97 ± 0.08*	2.01 ± 0.18*	4.08 ± 0.31*
CLP + CTXA (0.294 mg/kg)	219.09 ± 12.38*	24.18 ± 2.08*	0.92 ± 0.07*	1.98 ± 0.12*	4.02 ± 0.37*

Sham, sham-operated mice; aloin, mice treated with aloin (12.4 mg/kg body weight) at 12 and 50 h; CTXA, mice treated with CTXA (0.294 mg/kg body weight) at 12 and 50 h; CLP, CLP-operated mice; aloin + CLP, mice treated with aloin at 12 and 50 h after CLP surgery; CTXA + CLP, mice treated with CTXA at 12 and 50 h after CLP surgery.

* $p < 0.05$ as compared to CLP.

[a] Each value represents the mean ± SD (n = 10).

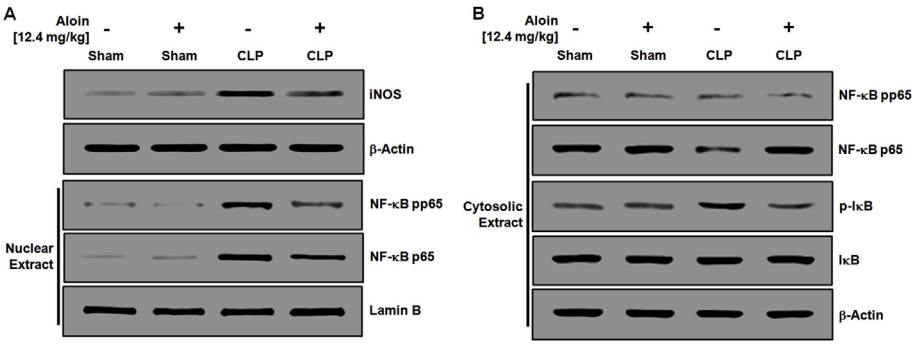

Fig. 2. Effects of aloin treatment on the expression levels of renal iNOS, IκB and NF-κB expression in CLP-operated mice. Sham, sham-operated mice; Sham + aloin, mice treated with aloin (12.4 mg/kg body weight) at 12 and 50 h after sham operation. CLP, CLP-operated mice; CLP + aloin, mice treated with aloin (12.4 mg/kg body weight) at 12 and 50 h after CLP surgery (from left line). Western blots of iNOS, phosphor-IκB, IκB, phosphor–NF–κB, NF-κB, Lamin-B, and β-actin. The image is representative of results obtained from three different experiments.

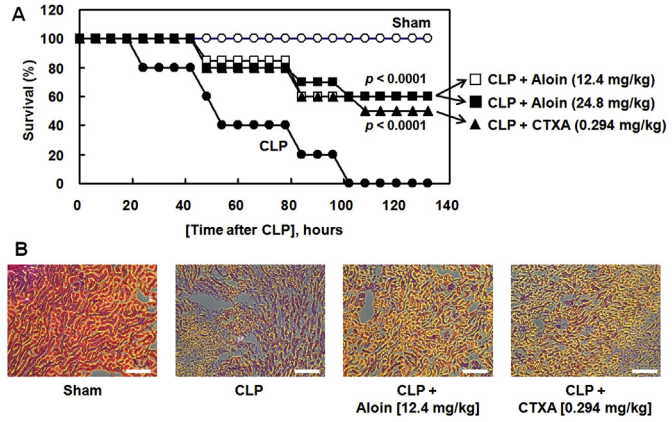

Fig. 3. Effects of aloin treatment on CLP-induced septic lethality and histopathological change in kidney tissues. Male C57BL/6 mice (n = 20) were administered aloin at 12.4 mg/kg (i.v. □), 24.8 mg/kg (i.v. ■), or CTXA (0.294 mg/kg, i.v. ▲) at 12 h and 50 h after CLP. (A) Animal survival was monitored every 12 h for 132 h after CLP. Control CLP mice (●) and sham-operated mice (○) were administered sterile saline (n = 20). Kaplan-Meier survival analysis was used to determine the overall survival rates versus CLP treated mice. (B) Histological examination of kidney sections from Sham control, CLP with or without aloin treated mice (H&E staining, original magnification 200×). The images are representative of three separate experiments conducted on different days with similar results. The scale bar represents 100 μm.

histological changes in kidney tissues. Systemic inflammation during sepsis frequently causes multiple organ failure, with the liver and kidney as the major target organs (Astiz and Rackow, 1998). Fig. 3B showed the renal histological changes in the Sham and CLP with or without aloin. Histological evaluation of the renal sections of mice in the Sham groups revealed a regular morphology of the glomeruli and tubuli (Fig. 3B). However, CLP induced tissue destruction proximal and distal tubules along with severe infiltration of polymorphonuclear leukocytes. In contrast, aloin post-treated CLP group was found to attenuate many of the symptoms of renal injury (Fig. 3B). These histological data confirmed the plasma levels of renal damage markers (Table 1).

4. Discussion

The aim of the present study was to evaluate the potential effects of aloin, an active compound isolated from *Aloe* species, on renal damage in mice with acute CLP-induced sepsis. Our data demonstrated that post-surgical treatment with aloin significantly ameliorated CLP-induced deterioration in renal function. Furthermore, aloin reduced the levels of TNF-α, IL-6, NO, and MPO that were elevated after CLP; additionally, aloin treatment reduced elevated iNOS levels after CLP surgery. These ameliorative effects were accompanied by an increase in the activities of antioxidant enzymes and a reduction in the levels of lipid peroxidation products in renal tissues, which was similar to the renal protective effects of couomarins from *Hydrangea paniculata* (HP) (Zhang et al., 2017). Extract of HP protect renal function in lipopolysaccharide-induced septic acute kidney injury by anti-inflammatory and antioxidant activities, and has potential in the critical care of septic acute kidney injury (Zhang et al., 2017). The underlying molecular mechanism of aloin's renal protective effects appeared to involve the suppression of NF-κB activation. Therefore, the results of the present study suggested that aloin might potentially have beneficial effects in therapies to prevent acute renal injury due to sepsis.

We found that excretion of urinary proteins and the levels of plasma BUN and creatinine were increased after CLP surgery; these findings are consistent with previous reports (Bhargava et al., 2013; Guo and Ward, 2006; Huber-Lang et al., 2001). Our study also found that changes in kidney function after CLP surgery could be ameliorated by aloin treatment, since significant reductions in BUN, creatinine, and urine protein levels were identified. NO is an important proinflammatory molecule that is released during inflammatory responses. In pathological conditions, iNOS is induced and then NO is synthesized, and can affect many parts of the inflammatory cascade (Cadenas and Cadenas, 2002). There is substantial evidence that CLP-mediated renal inflammatory damage may be due to increased iNOS activity and consequent abnormal NO levels (Draisma et al., 2010; Parratt, 1998; Symeonides and Balk, 1999). Our results showed that CLP-operated mice had enhanced NO production in blood and iNOS expression in kidney tissue; these changes were significantly reduced by treatment with aloin.

TNF-α and IL-6 are involved in CLP-induced tissue damage and are regarded as major regulators of severe inflammatory diseases such as sepsis or septic shock (Chaudhry et al., 2013; Stearns-Kurosawa et al., 2011). In this study, we found that aloin treatment reduced the levels of TNF-α and IL-6. Since the increased release of cytokines, particularly TNF-α and IL-6, appears to be an essential aspect of pathogenesis in the inflammation process, the inhibitory effects of aloin on CLP-induced TNF-α and IL-6 production might be a crucial step in the anti-inflammatory action of aloin. The nuclear transcription factor NF-κB amplifies and regulates many genes, including multiple cytokines and iNOS in response to inflammatory stimuli. When activated by such stimuli, NF-κB dissociates from IκB and translocates to the nucleus, leading to gene transcription (Oeckinghaus and Ghosh, 2009). NF-κB is a promising target for treating a variety of diseases because it plays a diverse role in the expression of inflammatory genes. In this study, aloin blocked the CLP-induced activation of NF-κB by inhibiting the degradation of IκB. These observations indicate that interference with NF-κB might explain, as least in part, the inhibitory effects of aloin on iNOS, TNF-α, and IL-6 levels. Similar to the renal protective effects of aloin, treatment of skimmin (one of the major pharmacologically active molecules present in HP) can significantly improve renal function by inhibiting IL-1β and IL-6 and regulating the levels of creatitine, urea nitrogen and albumin excretion (Zhang et al., 2013).

The antioxidant enzymes SOD, CAT, and GSH-Px are considered to be the primary defenses against oxidative damage in tissues (Birben

et al., 2012). Septic conditions have been found to impair the balance between free radical scavenging and production by cellular antioxidant systems (Hatwalne, 2012; Horton, 2003). Our data showed decreased levels of the three enzymes in kidney tissue in CLP-operated mice; the activities of these enzymes were significantly raised by aloin treatment. These results indicate that may have potential therapeutic value in oxidative stress-associated kidney diseases. The major lipid peroxidation product, MDA, is a good indicator of oxidative stress; a negative correlation has been reported between the MDA level and the activities of endogenous antioxidant enzymes (Qiao et al., 2011; Xiao et al., 2012; Zhang et al., 2011). Here, our data showed that renal MDA levels were increased in CLP-operated mice and that aloin treatment significantly reduced this increase. As described above, aloin may promote the activities and levels of SOD, CAT, and GSH-Px in kidney tissues of CLP mice. Therefore, our data indicate that aloin could provide renal protection against CLP-induced oxidative injury via inhibiting lipid peroxidation as well as promoting the activities and expression of endogenous antioxidant enzymes.

In conclusion, this study has demonstrated a renal protective effect by aloin against CLP-induced kidney injury and septic lethality. The ameliorative effects of aloin were associated with down-regulation of TNF-α and IL-6 production reduction of iNOS expression, and lowering of NO production by blocking the NF-κB pathway. These effects were accompanied by enhanced antioxidant defense and decreased lipid peroxidation in the kidney and plasma *in vivo*. Overall, our results suggest that although treatment with high doses of aloin (> 12.4 mg/kg) had no additional beneficial effects, aloin has the potential to be considered for therapeutic use in the treatment of renal inflammatory damage and sepsis-induced oxidative stress.Acknowledgements

This work was supported by the National Research Foundation of Korea grant funded by the Korea government (MSIT, 2017M3A9G8083382 and 2018R1A5A2025272).

Conflicts of interest

The authors have no conflict of interest to disclose.

Transparency document

Transparency document related to this article can be found online at https://doi.org/10.1016/j.fct.2019.110651.

References

Agca, C.A., Tuzcu, M., Hayirli, A., Sahin, K., 2014. Taurine ameliorates neuropathy via regulating NF-kappaB and Nrf2/HO-1 signaling cascades in diabetic rats. Food Chem. Toxicol. 71, 116–121.
Arosio, B., Gagliano, N., Fusaro, L.M., Parmeggiani, L., Tagliabue, J., Galetti, P., De Castri, D., Moscheni, C., Annoni, G., 2000. Aloe-Emodin quinone pretreatment reduces acute liver injury induced by carbon tetrachloride. Pharmacol. Toxicol. 87, 229–233.
Astiz, M.E., Rackow, E.C., 1998. Septic shock. Lancet 351, 1501–1505.
Beppu, H., Koike, T., Shimpo, K., Chihara, T., Hoshino, M., Ida, C., Kuzuya, H., 2003. Radical-scavenging effects of Aloe arborescens Miller on prevention of pancreatic islet B-cell destruction in rats. J. Ethnopharmacol. 89, 37–45.
Beutler, E., Duron, O., Kelly, B.M., 1963. Improved method for the determination of blood glutathione. J. Lab. Clin. Med. 61, 882–888.
Bhargava, R., Altmann, C.J., Andres-Hernando, A., Webb, R.G., Okamura, K., Yang, Y., Falk, S., Schmidt, E.P., Faubel, S., 2013. Acute lung injury and acute kidney injury are established by four hours in experimental sepsis and are improved with pre, but not post, sepsis administration of TNF-alpha antibodies. PLoS One 8, e79037.
Birben, E., Sahiner, U.M., Sackesen, C., Erzurum, S., Kalayci, O., 2012. Oxidative stress and antioxidant defense. World Allergy Organ J 5, 9–19.
Buras, J.A., Holzmann, B., Sitkovsky, M., 2005. Animal models of sepsis: setting the stage. Nat. Rev. Drug Discov. 4, 854–865.
Cadenas, S., Cadenas, A.M., 2002. Fighting the stranger-antioxidant protection against endotoxin toxicity. Toxicology 180, 45–63.
Chaudhry, H., Zhou, J., Zhong, Y., Ali, M.M., McGuire, F., Nagarkatti, P.S., Nagarkatti, M., 2013. Role of cytokines as a double-edged sword in sepsis. In Vivo 27, 669–684.
Chen, S.H., Lin, K.Y., Chang, C.C., Fang, C.L., Lin, C.P., 2007. Aloe-emodin-induced apoptosis in human gastric carcinoma cells. Food Chem. Toxicol. 45, 2296–2303.
Diehl, K.H., Hull, R., Morton, D., Pfister, R., Rabemampianina, Y., Smith, D., Vidal, J.M., van de Vorstenbosch, C., 2001. A good practice guide to the administration of substances and removal of blood, including routes and volumes. J. Appl. Toxicol. 21, 15–23.
Doi, K., Leelahavanichkul, A., Yuen, P.S., Star, R.A., 2009. Animal models of sepsis and sepsis-induced kidney injury. J. Clin. Investig. 119, 2868–2878.
Draisma, A., Dorresteijn, M.J., Bouw, M.P., van der Hoeven, J.G., Pickkers, P., 2010. The role of cytokines and inducible nitric oxide synthase in endotoxemia-induced endothelial dysfunction. J. Cardiovasc. Pharmacol. 55, 595–600.
Esmat, A.Y., El-Gerzawy, S.M., Rafaat, A., 2005. DNA ploidy and S phase fraction of breast and ovarian tumor cells treated with a natural anthracycline analog (aloin). Cancer Biol. Ther. 4, 108–112.
Esmat, A.Y., Tomasetto, C., Rio, M.C., 2006. Cytotoxicity of a natural anthraquinone (Aloin) against human breast cancer cell lines with and without ErbB-2: topoisomerase IIalpha coamplification. Cancer Biol. Ther. 5, 97–103.
Guo, R.F., Ward, P.A., 2006. C5a, a therapeutic target in sepsis. Recent Pat. Anti-Infect. Drug Discov. 1, 57–65.
Hatwalne, M.S., 2012. Free radical scavengers in anaesthesiology and critical care. Indian J. Anaesth. 56, 227–233.
Horton, J.W., 2003. Free radicals and lipid peroxidation mediated injury in burn trauma: the role of antioxidant therapy. Toxicology 189, 75–88.
Huber-Lang, M., Sarma, V.J., Lu, K.T., McGuire, S.R., Padgaonkar, V.A., Guo, R.F., Younkin, E.M., Kunkel, R.G., Ding, J., Erickson, R., Curnutte, J.T., Ward, P.A., 2001. Role of C5a in multiorgan failure during sepsis. J. Immunol. 166, 1193–1199.
Kim, J.E., Lee, W., Yang, S., Cho, S.H., Baek, M.C., Song, G.Y., Bae, J.S., 2019. Suppressive effects of rare ginsenosides, Rk1 and Rg5, on HMGB1-mediated septic responses. Food Chem. Toxicol. 124, 45–53.
Lam, R.Y.Y., Woo, A.Y.H., Leung, P.S., Cheng, C.H.K., 2007. Antioxidant actions of phenolic compounds found in dietary plants on low-density lipoprotein and erythrocytes in vitro. J. Am. Coll. Nutr. 26, 233–242.
Lee, I.C., Bae, J.S., 2019. Pelargonidin protects against renal injury in a mouse model of sepsis. J. Med. Food 22, 57–61.
Lee, W., Lee, Y., Jeong, G.S., Ku, S.K., Bae, J.S., 2017. Cudratricusxanthone A attenuates renal injury in septic mice. Food Chem. Toxicol. 106, 404–410.
Lee, W., Yang, S., Lee, C., Park, E.K., Kim, K.M., Ku, S.K., Bae, J.S., 2019. Aloin reduces inflammatory gene iNOS via inhibition activity and p-STAT-1 and NF-kappaB. Food Chem. Toxicol. 126, 67–71.
Li, S.W., Yang, T.C., Lai, C.C., Huang, S.H., Liao, J.M., Wan, L., Lin, Y.J., Lin, C.W., 2014. Antiviral activity of aloe-emodin against influenza A virus via galectin-3 up-regulation. Eur. J. Pharmacol. 738, 125–132.
Lin, C.W., Wu, C.F., Hsiao, N.W., Chang, C.Y., Li, S.W., Wan, L., Lin, Y.J., Lin, W.Y., 2008. Aloe-emodin is an interferon-inducing agent with antiviral activity against Japanese encephalitis virus and enterovirus 71. Int. J. Antimicrob. Agents 32, 355–359.
Lu, A.P., Jia, H.W., Xiao, C., Lu, Q.P., 2004. Theory of traditional Chinese medicine and therapeutic method of diseases. World J. Gastroenterol. 10, 1854–1856.
Luo, X., Zhang, H., Wei, X., Shi, M., Fan, P., Xie, W., Zhang, Y., Xu, N., 2018. Aloin suppresses lipopolysaccharide-induced inflammatory response and apoptosis by inhibiting the activation of NF-kappaB. Molecules 23.
Miranda, K.M., Espey, M.G., Wink, D.A., 2001. A rapid, simple spectrophotometric method for simultaneous detection of nitrate and nitrite. Nitric Oxide 5, 62–71.
Niciforovic, A., Adzic, M., Spasic, S.D., Radojcic, M.B., 2007. Antitumor effects of a natural anthracycline analog (Aloin) involve altered activity of antioxidant enzymes in HeLaS3 cells. Cancer Biol. Ther. 6, 1200–1205.
Oeckinghaus, A., Ghosh, S., 2009. The NF-kappaB family of transcription factors and its regulation. Cold Spring Harb Perspect Biol 1 a000034.
Ozdulger, A., Cinel, I., Koksel, O., Cinel, L., Avlan, D., Unlu, A., Okcu, H., Dikmengil, M., Oral, U., 2003. The protective effect of N-acetylcysteine on apoptotic lung injury in cecal ligation and puncture-induced sepsis model. Shock 19, 366–372.
Park, M.Y., Kwon, H.J., Sung, M.K., 2009. Evaluation of aloin and aloe-emodin as anti-inflammatory agents in aloe by using murine macrophages. Biosc. Biotech. Biochem. 73, 828–832.
Parratt, J.R., 1998. Nitric oxide in sepsis and endotoxaemia. J. Antimicrob. Chemother. 41 (Suppl. A), 31–39.
Qiao, Y., Bai, X.F., Du, Y.G., 2011. Chitosan oligosaccharides protect mice from LPS challenge by attenuation of inflammation and oxidative stress. Int. Immunopharmacol. 11, 121–127.
Russell, J.A., 2006. Management of sepsis. N. Engl. J. Med. 355, 1699–1713.
Seo, E., Lee, E.K., Lee, C.S., Chun, K.H., Lee, M.Y., Jun, H.S., 2014. Psoralea corylifolia L. seed extract ameliorates streptozotocin-induced diabetes in mice by inhibition of oxidative stress. Oxid Med Cell Longev 2014, 897296.
Silva, M.A., Trevisan, G., Hoffmeister, C., Rossato, M.F., Boligon, A.A., Walker, C.I., Klafke, J.Z., Oliveira, S.M., Silva, C.R., Athayde, M.L., Ferreira, J., 2014. Anti-inflammatory and antioxidant effects of Aloe saponaria Haw in a model of UVB-induced paw sunburn in rats. J. Photochem. Photobiol., B 133, 47–54.
Singer, M., Deutschman, C.S., Seymour, C.W., Shankar-Hari, M., Annane, D., Bauer, M., Bellomo, R., Bernard, G.R., Chiche, J.D., Coopersmith, C.M., Hotchkiss, R.S., Levy, M.M., Marshall, J.C., Martin, G.S., Opal, S.M., Rubenfeld, G.D., van der Poll, T., Vincent, J.L., Angus, D.C., 2016. The third international consensus definitions for sepsis and septic shock (Sepsis-3). J. Am. Med. Assoc. 315, 801–810.
Stearns-Kurosawa, D.J., Osuchowski, M.F., Valentine, C., Kurosawa, S., Remick, D.G., 2011. The pathogenesis of sepsis. Annu. Rev. Pathol. 6, 19–48.
Symeonides, S., Balk, R.A., 1999. Nitric oxide in the pathogenesis of sepsis. Infect. Dis. Clin. N. Am. 13, 449–463 (x).
Tabolacci, C., Lentini, A., Mattioli, P., Provenzano, B., Oliverio, S., Carlomosti, F., Beninati, S., 2010. Antitumor properties of aloe-emodin and induction of transglutaminase 2 activity in B16-F10 melanoma cells. Life Sci. 87, 316–324.
Tao, L., Xie, J., Wang, Y., Wang, S., Wu, S., Wang, Q., Ding, H., 2014. Protective effects of aloe-emodin on scopolamine-induced memory impairment in mice and H(2)O(2)-

induced cytotoxicity in PC12 cells. Bioorg. Med. Chem. Lett 24, 5385–5389.
Vincent, J.L., Zhang, H., Szabo, C., Preiser, J.C., 2000. Effects of nitric oxide in septic shock. Am. J. Respir. Crit. Care Med. 161, 1781–1785.
Wan, L., Zhang, L., Fan, K., Wang, J., 2017. Aloin promotes A549 cell apoptosis via the reactive oxygen speciesmitogen activated protein kinase signaling pathway and p53 phosphorylation. Mol. Med. Rep. 16, 5759–5768.
Woo, S.W., Nan, J.X., Lee, S.H., Park, E.J., Zhao, Y.Z., Sohn, D.H., 2002. Aloe emodin suppresses myofibroblastic differentiation of rat hepatic stellate cells in primary culture. Pharmacol. Toxicol. 90, 193–198.
Xiao, J.H., Xiao, D.M., Chen, D.X., Xiao, Y., Liang, Z.Q., Zhong, J.J., 2012. Polysaccharides from the medicinal mushroom cordyceps taii show antioxidant and immunoenhancing activities in a D-galactose-induced aging mouse model. Evid. Based Complement Altern. Med. 2012, 273435. https://www.hindawi.com/journals/ecam/2012/273435/.
Yu, C.S., Yu, F.S., Chan, J.K., Li, T.M., Lin, S.S., Chen, S.C., Hsia, T.C., Chang, Y.H., Chung, J.G., 2006. Aloe-emodin affects the levels of cytokines and functions of leukocytes from Sprague-Dawley rats. In Vivo 20, 505–509.
Yu, M., Xu, M., Liu, Y., Yang, W., Rong, Y., Yao, P., Yan, H., Wang, D., Liu, L., 2013. Nrf2/ARE is the potential pathway to protect Sprague-Dawley rats against oxidative stress induced by quinocetone. Regul. Toxicol. Pharmacol. 66, 279–285.
Zhang, J., Yu, Y., Zhang, Z., Ding, Y., Dai, X., Li, Y., 2011. Effect of polysaccharide from cultured Cordyceps sinensis on immune function and anti-oxidation activity of mice exposed to 60Co. Int. Immunopharmacol. 11, 2251–2257.
Zhang, S., Ma, J., Sheng, L., Zhang, D.M., Chen, X.G., Yang, J.Z., Wang, D.J., 2017. Total coumarins from Hydrangea paniculata show renal protective effects in lipopolysaccharide-induced acute kidney injury via anti-inflammatory and antioxidant activities. Front. Pharmacol. 8.
Zhang, S., Xin, H.Q., Li, Y., Zhang, D.M., Shi, J., Yang, J.Z., Chen, X.G., 2013. Skimmin, a coumarin from Hydrangea paniculata, slows down the progression of membranous glomerulonephritis by anti-inflammatory effects and inhibiting immune complex deposition. Evid. Based Complement Altern. Med. 2013, 1–10. https://doi.org/10.1155/2.13/413237.